Shear Tests on Rubble Stone Masonry Panels - Diagonal Compression Tests

J. Milosevic, R. Bento, A. S. Gago & M. Lopes
ICIST, IST, Technical University of Lisbon, Portugal

SUMMARY
Rubble stone masonry walls with lime mortars are typical of Portuguese traditional construction, but can be seen in other Mediterranean countries. It is accepted that the seismic resistance of those masonry buildings is low, but little was done to characterize experimentally the shear strength of the masonry walls. This paper describes the experimental campaign carried out to obtain the shear strength and the shear modulus of the Lisbon traditional masonry (external) walls. The tests were performed according to the ASTM E519-02 standard and were numerically simulated by nonlinear finite element models (smeared crack concept) and discrete element models. Diagonal compression tests were performed in four lime stone specimens: two specimens were built with air lime, and for two other specimens hydraulic mortar was used. Based on experimental results the nonlinear numerical models were calibrated, showing that load-displacement diagrams and failure modes obtained numerically have a good agreement with the results obtained in the experimental tests.

Keywords: rubble masonry buildings, diagonal compression test, numerical analysis

1. INTRODUCTION

Old buildings with load bearing masonry walls are an important percentage of Lisbon building stock. Those buildings were built during the XVIII century Lisbon reconstruction, after the 1755 earthquake ("Pombalinos" buildings) [Cardoso et al., 2005], or during the Lisbon expansion on the late XIX century ("Gaioleiros" buildings) [Mendes & Lourenço, 2010]. The internal walls of these two types of buildings show different typologies and arrangements, but the external walls are similar, built with identical materials and similar construction techniques (rubble stone masonry).

In order to simulate the buildings structural behavior it is necessary to know the mechanical characteristics of the materials, for any numerical analysis. However, experimental data about materials mechanical properties is still missing, especially what regards the shear strength parameters, and thus experimental campaigns should be done in order to support the numerical and analytical models.

Within of the research project SEVERES (www.severes.org) four rubble stone masonry specimens were built and tested, aiming to characterize the shear strength of rubble stone masonry. These tests consist of diagonal compression test, which is described in this paper. For these tests four masonry specimens ($120 \times 120 \times 70$ cm) were built with two types of mortar; two were built with air lime mortar (W2 and W3), whereas the remaining two specimens were constructed with hydraulic lime mortar (W1 and W4). The diagonal compression tests followed, as much as possible, the ASTM E519-02 standards [ASTM, 2002] and other similar work where rubble stone masonry walls were also tested [Corradi et al., 2003, Brignola et al., 2008].

Furthermore, based on experimental results nonlinear finite element models (smeared crack approach) and distinct element models were calibrated by means of DIANA [Diana, 2005] and UDEC [Itasca, 2011] computer codes, respectively.

2. DIAGONAL COMPRESSION TEST

2.1 Test description

Diagonal compression tests were performed in four masonry specimens ($120 \times 120 \times 70$ cm) in order to obtain the diagonal tensile (shear) strength and shear modulus. As referred, two masonry specimens were built with air lime mortar (specimens W2 and W3), whereas the other two specimens were based on hydraulic lime mortar (specimens W1 and W4). All panels were built in the laboratory following the techniques and materials typical of Portuguese masonry buildings and tested eight months after its construction to ensure the hardness of the mortars.

These tests panels were positioned in the testing machine with a diagonal axis in the vertical direction and loaded in compression along this direction (Fig. 2.1). According to the ASTM standard [ASTM, 2002], test setup is composed of two steel loading shoes, which were fixed on two opposite corners of a diagonal of the masonry specimens, as in shown in Fig.2.1.

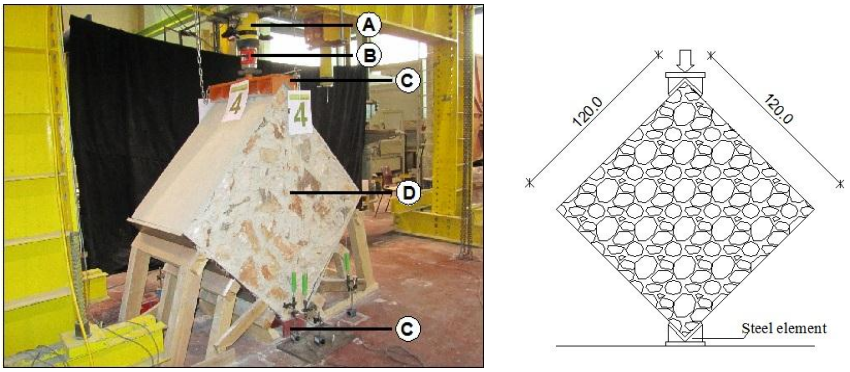

Figure 2.1. Test setup for diagonal compression test (dimension in [cm])
A – Hydraulic jack; B – Load cell; C – Loading shoes; D – Masonry specimen

For both type of masonry specimens, with hydraulic and air lime mortar, the load was applied gradually with increments rates of 10 kN/s. In order to measure the shortening of the vertical diagonal and the lengthening of the horizontal diagonal linear displacement transducers (TSV and TSH, respectively) were placed on both sides of the specimens. The number of transducers which were used for each specimen was eight, five transducers were connected on one side and the remaining three transducers were placed on the other side of the specimens, as can be seen in Fig. 2.2. Moreover, one transducer was placed under the hydraulic jack in order to measure vertical displacement. When the behavior of the specimen under load indicates it might be close of failure, the transducers were removed in order to avoid any damage of the instrumentation. After that, until the collapse of the specimen, the load was continuously applied.

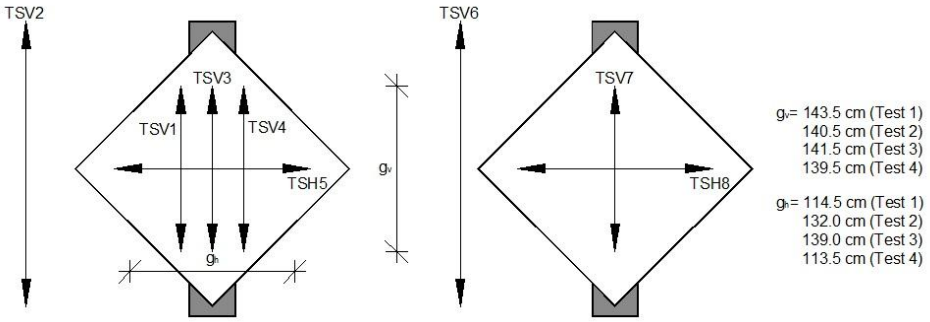

(a) (b)

Figure 2.2. Position of transducers: (a) wall front side; (b) wall back side (dimension in [cm])

Following the ASTM [ASTM, 2002] standard, the shear stress τ and shear elastic modulus (or modulus of rigidity) G for specimens are calculated from the experimental test. In this case the Mohr's circle is centered in the origin of the Cartesian system of axis and the value of the shear stress τ is equal to the principal tensile stress f_t. The shear stress τ is obtained by means of Eqn. 2.1.

$$\tau = \frac{0.707 \times P}{A_n} \tag{2.1}$$

where P is the load applied by the jack and A_n is the net area of the specimen, calculated as follows:

$$A_n = \left(\frac{w+h}{2} \right) \times t \times n \tag{2.2}$$

where w is the specimen width, h is the specimen height, t is the thickness of the specimen and n is the percentage of the unit's gross area that is solid, expressed as a decimal. In this work the value n =1 was adopted.

Consequently, the initial shear strength τ_0 (f_{v0} according to Eurocode 6 [EC 6, 1995]) and the tensile strength are defined as:

$$\tau_0 = f_t = \frac{0.707 \times P_{\max}}{A_n} \tag{2.3}$$

where $P_{\max}$ is the maximum load applied by the jack.

Furthermore, shear elastic modulus G is obtained by:

$$G = \frac{\tau_{1/3}}{\gamma_{1/3}} \tag{2.4}$$

where $\tau_{1/3}$ is the shear stress for a load of 1/3 of the maximum load $P_{\max}$ and $\gamma_{1/3}$ is the corresponding shear strain.

2.2 Experimental Results of Diagonal Compression Tests

2.2.1 Failure modes

Experimental results, which were obtained in this experimental campaign, showed that all specimens have similar failure patterns. Failure pattern for specimen based on hydraulic mortar (W4) and specimen based on air lime mortar (W3) can be seen in Fig. 2.3. It is worth noting that in all specimens a main crack started in the middle of the specimens, spreading (developing) towards the upper and the bottom corners (only through the mortar, without damaging the stones), causing the collapse.

(a) (b)

Figure 2.3. Main crack at the middle of the specimens: (a) specimen W4 and (b) specimen W3

Due to different mechanical properties of mortar, the specimens showed different behavior at the collapse, namely the walls W2 and W3, which were based on air lime mortar, were disintegrated after the collapse, while the walls with hydraulic mortar, W1 and W4, were divided in two almost symmetrical parts, as in shown in Fig. 2.4.

(a) (b)

Figure 2.4. Collapse of masonry specimens: (a) specimen W4 and (b) specimen W3

2.2.2. Masonry Specimens Based on Hydraulic Lime Mortar

The load-vertical displacement diagram, which is shown in Fig. 2.5 (where vertical displacement represents average values of the measurement recorded using LVDTs 3 and 7) showed that maximum load for specimens W1 was 372 kN, with vertical shortening of 1.55 mm (Point 1), but in this case the collapse of specimen occurred later with a load value of 268 kN and vertical shortening of 5.29 mm

(Point 2). In specimen W4 the point on the collapse was the one at which the maximum load was applied, with a magnitude of 306 kN and a vertical displacement of 3.47 mm (Point 3).

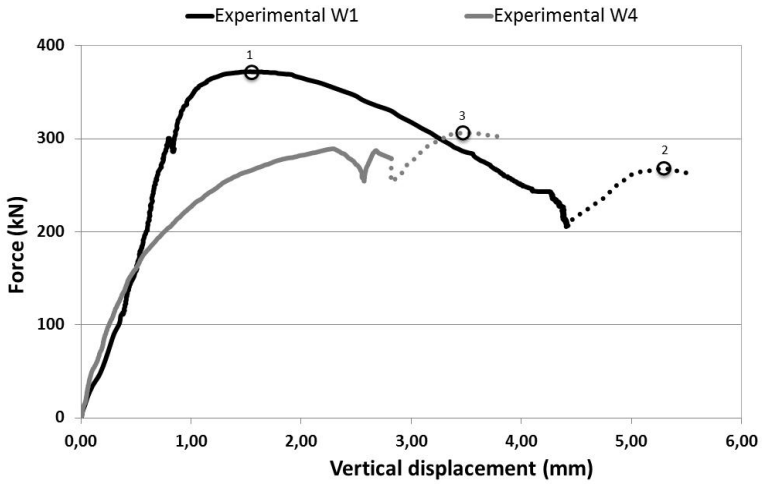

Figure 2.5. Walls W1 and W4: Force vs. Vertical displacement (Note: vertical displacement measured at the top of the specimens)

The main reason for apparent ductile behavior of wall W1 is that the specimen W1 was built with horizontal stone layers, whereas the other three specimens, in order to represent real masonry walls in Portugal, were built with diagonal layers (45º).

As already mentioned, all transducers (except the transducer that was placed under the hydraulic jack) were removed before the end of test, for safety reason. In order to define the complete behavior of the walls, the dotted parts of the curves in Fig. 2.5 and Fig. 2.6 (which is shown in the following) were obtained by interpolation using the measurement of the transducers under the hydraulic jack.

2.2.3. Masonry Specimens Based on Air Lime Mortar

According to the obtained experimental results can be concluded that the masonry specimens with air lime mortar have much lower strength, comparing to the specimens based on hydraulic lime mortar. In Figure 2.6 can be seen that the collapse load for wall W2 was 29 kN, with a vertical displacement of 1.58 mm (Point 1), and for specimen W3 the ultimate load was 28 kN with vertical shortening of 1.52 mm (Point 2), where the vertical displacement represents average values of the measurement recorded using LVDTs 3 and 7.

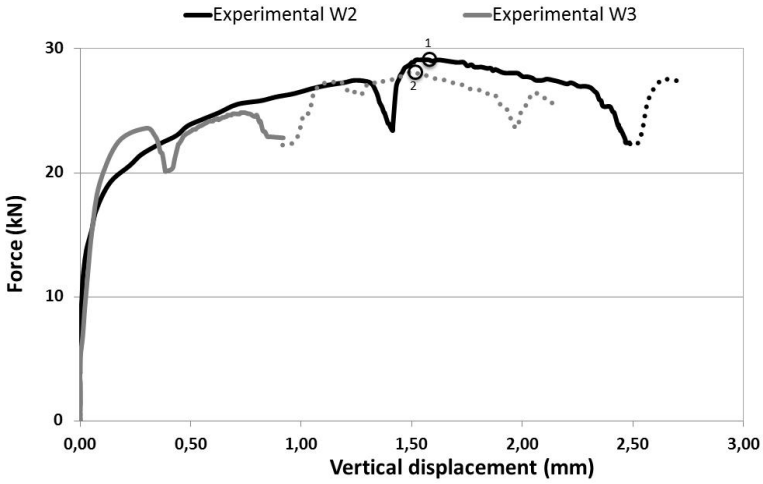

Figure 2.6. Walls W2 and W3: Force vs. Vertical displacement (Note: vertical displacement measured at the top of the specimens)

In Table 2.1 the summarized results obtained by diagonal compression tests are summarized.

Table 2.1. Results of Diagonal Compression Tests

Masonry typology	Masonry Specimen	P_{max} [kN]	$\tau_0 = f_t$ [MPa]	G [MPa]
Rubble Stone Masonry Specimens	W1	372	0.313	389.3
	W2	29	0.024	57.9
	W3	28	0.024	92.5
	W4	306	0.258	252.0

2.3 Discussion

The first conclusion, which can be obtained from the experimental results, is that the wall shear strength is dependent on the mortar resistance, since the cracks propagated mainly through the joints, without damaging the stones. Based on the experimental results, it is noticed that the stone arrangement also leads to some differences in masonry strength, but especially on the deformation capacity. However, the influence of the stone is not as important as the influence of the type of mortar, which is very high: specimens with air lime mortar showed much lower shear strength (about 10 times) than the specimens built with hydraulic mortar. Moreover, differences between the values of the shear modulus G (as referred, G is measured in the elastic regime, for 1/3 of the maximum load) also depend on the type of mortar, as in shown in Table 2.1. Moreover, the shear modulus values present a significant variation between the specimens with the same type of mortar. The variation of shear modulus (G) for air lime mortar specimens is about 38% and 35% for hydraulic lime mortar specimens. This variation can be explained by the fact that the shear modulus is evaluated on the undamaged stage, corresponding to small displacements, where measurement errors may have an important influence. The variation of the shear modulus G between specimens with hydraulic lime mortar can also be explained by the different stone arrangement adopted (W1 with horizontal and W4 with diagonal layers).

3. NUMERICAL MODELING

In the present work two types of numerical models were used to simulate the diagonal compression tests, namely nonlinear finite element models [Diana, 2005] and distinct element models [Itasca, 2011]. In the case of rubble stone masonry walls, position of the crack cannot be defined in advance and, due to this fact, in the finite element models the cracking of masonry was simulated by a smeared crack approach. The distinct element method allows the explicit modeling of stones and mortar joints, with displacement and rotations of the individual blocks, thus it allows the investigation of the failure mechanism of stone masonry buildings. In order to reproduce the arbitrary stone arrangements in the masonry specimens and made possible the use of distinct element method for rubble stone masonry specimens, the Voronoi [Klein, 1989] algorithm was used.

3.1 Nonlinear Finite Element Model

The non-linear behavior of the rubble masonry units was represented by a Total Strain Crack Model [Diana, 2005], based on a fixed stress-strain law concept. It describes that stress-strain relations are evaluated in a coordinate system that is fixed upon crack initiation. The panel is modeled with eight-node isoparametric plane stress elements (Fig. 3.7) and nonlinear geometric effects were not considered in the numerical simulations.

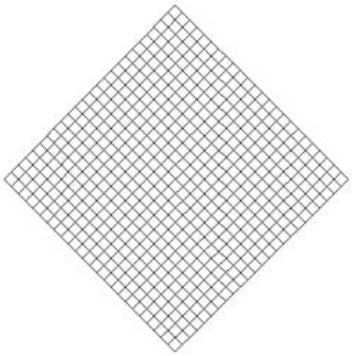

Figure 3.7. Finite element model mesh

The mechanical properties need to describe this material model are density (ρ =1835 kg/m^3), Young modulus (E = 3.27 GPa), the Poisson's ratio (ν = 0.20), the tensile strength (f_t =0.15 MPa and f_t =0.01 MPa, for hydraulic and air lime mortar, respectively), the fracture energy (G_{f1} = 100 N/m) and the shear retention factor (β = 0.1).

In numerical modeling the monotonic loads were applied on the specimens and the vertical load, which was applied at the top of the specimen, as in case of the experiments, was incrementally increased until the failure of the specimen. A displacement controlled procedure was applied to impose the load up to the failure, using the regular Newton-Raphson iteration procedure.

According to the results obtained with the finite element method, which are shown in Fig. 3.8 and Fig. 3.9, a reasonable matching between numerical and experimental values for both the ultimate load and the initial loading branch are obtained. Concerning the failure mode, the both numerical models, agrees reasonably well with the experimental results for both type of mortar. As shown in Fig. 3.10(a) and (b) and Fig. 3.11(a) and (b), the numerical results represented similar crack patterns developed during the experimental behavior of the wall, namely the diagonal cracking. Fig. 3.8 and Fig. 3.9 also show the ultimate load obtained by the distinct element method referred in the following section 3.2.

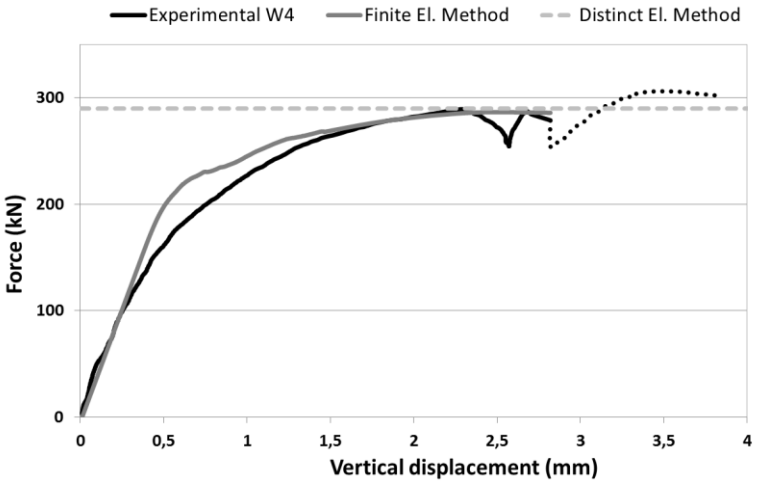

Figure 3.8. Experimental and numerical results: Force vs. Vertical displacement (Wall W4)

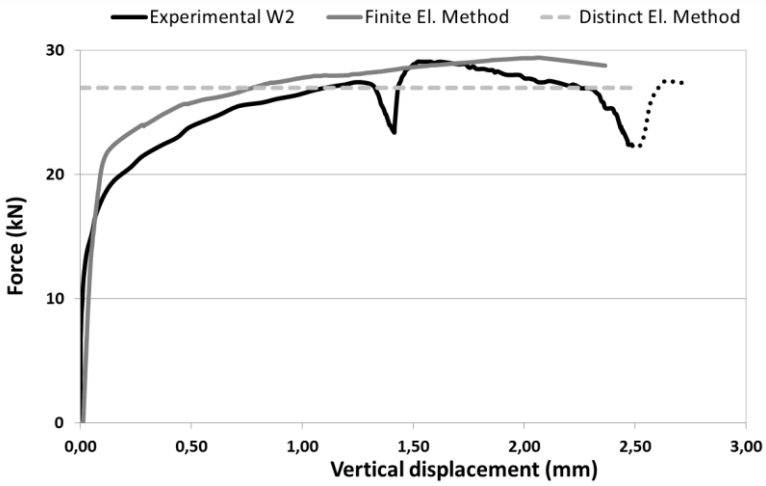

Figure 3.9. Experimental and numerical results: Force vs. Vertical displacement (Wall W2)

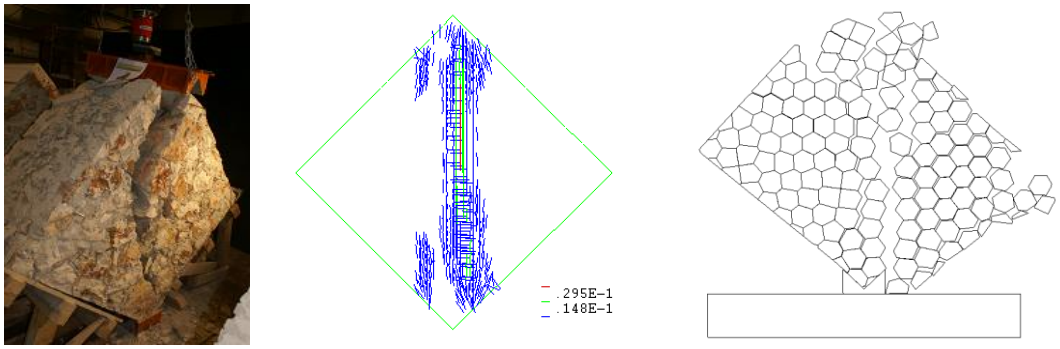

(a) (b) (c)

Figure 3.10. Wall W4 – Experimental and numerical failure modes: (a) Experimental; (c) Finite element model; (c) Distinct element model (in these pictures wall immediatley before collapse can be seen)

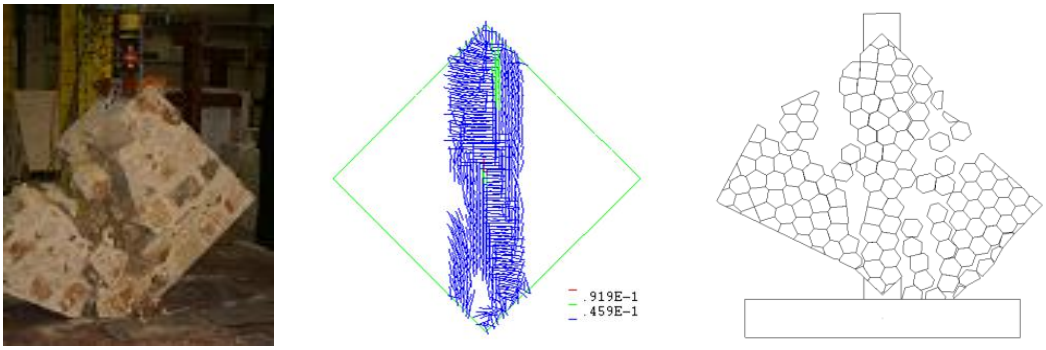

(a) (b) (c)

Figure 3.11. Wall W2 – Experimental and numerical failure modes: (a) Experimental; (c) Finite element model; (c) Distinct element model (in these pictures wall immediatley before collapse can be seen)

3.2 Distinct Element Model

The corresponding distinct element models of the specimen consisted in group of blocks elements, represented as randomly sized polygonal blocks, generated by an automatic joint generator, as shown in Fig. 3.12, where each block simulates a stone and was modeled by a finite difference elements mesh with linear elastic behavior (bulk modulus K=410 MPa and shear modulus G=450 MPa). An appropriate behavior was assigned to the contact between the blocks using a Coulomb slip model. The

parameters that control the contact behavior are the normal stiffness (J_{kn} =17 GPa and J_{kn} =8 Gpa for hydraulic and air lime mortar, respectively), the shear stiffness (J_{ks} =17 GPa and J_{ks} =8 GPa, for hydraulic and air lime mortar, respectively), the friction angle (ϕ =45º, for both type of mortar), the cohesion (c=0.23 MPa and c=0.03, for hydraulic and air lime mortar, respectively) and the tensile strength (f_t =0.23 MPa for hydraulic mortar and f_t =0.03 MPa for air lime mortar). It worth to refer that joint deformability parameters (J_{kn} and J_{ks}) control the initial loading branch and the joint strength parameters (ϕ , c and f_t) control the ultimate force level. Those values were quantified based on values adopted in other works [Gago et al., 2011, Azevedo et al., 2000] and the calibration of the numerical and experimental results.

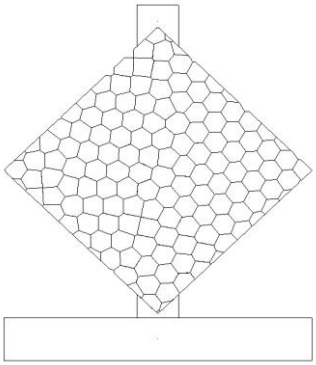

Figure 3.12. Randomly sized polygonal blocks

The numerical results which were obtained with the distinct element model for specimens based on hydraulic and air lime mortar is shown in Fig. 3.8 and Fig. 3.9, respectively and the corresponding collapse mode for both type of mortar can be seen in Fig. 3.10(c) and Fig. 3.11(c), respectively. As can be noticed a good matching between numerical and experimental values was achieved for the ultimate load and for the collapse pattern.

3.3 Discussion

In the present paper, force-displacement diagrams and failure modes were the main aspects under analysis. For both type of models, finite element and distinct element models, the good matching between numerical and experimental results for the ultimate load were obtained. Also, crack patterns, which were obtained by numerical analyses, were similar to crack patterns obtained by experimental results. As can be noticed, the good agreement between experimental results and results obtained by finite element model in sense of the initial branch of the load-displacement curve was achieved. In the distinct element analysis this curve cannot be obtained, at least not directly, which represents an advantage of the finite element method.

Since in rubble stone masonry walls, potential crack cannot be defined in advance, the smeared crack approach is more appropriate for modeling stone masonry panels, comparing with distinct element method. However, the use of the Voronoi algorithm to randomly generate the blocks in the distinct element model allows the use of a distinct methodology in a smeared sense.

4. CONCLUSIONS

As mentioned, the experimental work that were performed in this paper, allowed an evaluation of the shear strength and shear modulus of masonry via diagonal compression test for typical masonry walls

of old buildings in Portugal. Masonry panels (two with hydraulic and two with air lime mortar) were specially built for this experimental campaign.
According to the obtained experimental results, can be concluded that all tested masonry specimens have fragile behavior, but in the case of the specimens based on air lime mortar lower values of the shear strength were obtained, as expected. Namely, shear strength for air lime mortar is τ_0=0.024 MPa, whereas for specimens based on hydraulic lime shear strength reached τ_0=0.313 MPa and τ_0=0.258 MPa. It worth noting that mortar composition has an important influence on the shear strength. The experimental results for shear strength, which were obtained for air lime mortar, are corresponding to values of the Italian Standard [OPCM 3274, 2003].

Numerical analysis was performed by finite element models (smeared crack approach) and distinct element models, which are able to simulate the masonry behavior in shear. Both performed numerical analysis were shown results with a good matching to the experimental results in a sense of ultimate load and collapse pattern. It is important to say, that with the finite element models complete load-displacement curve was obtained, whereas with the distinct element method only the maximum applied load can be obtained. The simulation of rubble stone masonry panels by the distinct element method was achieved due to the use of the Voronoi algorithm in the blocks generation.

ACKNOWLEDGMENTS
The authors acknowledge the financial contribution of the FCT (*Fundação para a Ciência e a Tecnologia*) research project SEVERES: "Seismic Vulnerability of Old Masonry Buildings*"*.

REFERENCES

Cardoso, R., Lopes, M. L., Bento, R. (2005). Seismic Evaluation of Old Masonry Buildings. Part I: Method Description and Application to a Case-Study. *Journal of Engineering Structures* **27**, 2024–2035.

Mendes, N., Lourenço, P. B. (2010). Seismic Assessment of Masonry "Gaioleiro" Buildings in Lisbon, Portugal. *Journal of Earthquake Engineering* **14:1**, 80-101.

ASTM (2002). ASTM E 519-02, Standard Test Method for Diagonal Tension (Shear) in Masonry Assemblages. *ASTM International, West Conshohocken, PA*

Corradi, M., Borri, A., Vignoli, A. (2003). Experimental study on the determination of strength of masonry walls. *Journal of Construction and Building Materials* **17:5**, 325–337.

Brignola, A., Frumento, S., Lagomarsino, S., Podestà, S. (2008). Identification of shear parameters of masonry panels through the in-situ diagonal compression test. *International Journal of Architectural Heritage* **3:1**, 52–73.

DIANA (2005). DIsplacement method ANAlyser, release 9.1 [CD–ROM]. *Delft, The Netherlands: TNO DIANA BV.*

ITASCA (2011): UDEC version 4.01 - User's guide. *Itasca Consulting Group, Inc., Minneapolis, USA*

EC 6 (1995). Eurocode 6 - Design of masonry structures, part 1-1: general rules for buildings - rules for reinforced and unreinforced masonry. *ENV 1996-1-1:1995.*

Klein, R. (1989). Concrete and Abstract Voronoi Diagrams. *Lecture Notes in Computer Science. Springer-Verlag* **400**.

Gago, A. S., Alfaiate, J., Lamas, A. (2011). The effect of the infill in arched structures: Analytical and numerical modeling. *Journal of Engineering Structures* **33:5**, 1450-1458.

Azevedo, J., Sincraian, G., Lemos, J. V. (2000). Seismic behavior of blocky masonry structures. *Journal of Earthquake Spectra* **16:2**, 337-365.

OPCM 3274 (2003). Ordinanza del Presidente del Consiglio dei Ministri nº 3274 del 20 Marzo 2003: Allegato 2: - *Norme tecniche per il progetto, la valutazione e l'adeguamento sismico degli edifici, Italy*